Synthesis, Characterization, and Antibacterial Activity of Plant-Derived Zinc Oxide Nanostructure Using *Lavandula angustifolia* and *Phyllanthus niruri* Extracts

Dhiya Fakhirah[1], Tya Aisha Maghfira[1], Aulia Sukma Hutama[1], Abdi Wira Septama[2], Faiza Maryani[3], and Fransiska Sri Herwahyu Krismastuti[3*]

[1]*Department of Chemistry, Faculty of Mathematics and Natural Sciences, Universitas Gadjah Mada, Sekip Utara, Yogyakarta 55281, Indonesia*

[2]*Research Center for Pharmaceutical Ingredients and Traditional Medicine, National Research and Innovation Agency (BRIN), KST BJ Habibie, Setu, Tangerang Selatan 15314, Indonesia*

[3]*Research Center for Chemistry, National Research and Innovation Agency (BRIN), KST BJ Habibie, Setu, Tangerang Selatan 15314, Indonesia*

Corresponding author:

email: fran005@brin.go.id

Received: January 18, 2024
Accepted: March 4, 2024

DOI: 10.22146/ijc.93293

Abstract: *In recent years, green synthesized nanomaterials have garnered wide interest due to its inherent features like rapidity, cost-effectiveness, and environmentally friendly technique. The green synthesis of Zinc oxide nanostructures (n-ZnO) using two kinds of plant extract, lavender (*Lavandula angustifolia*) and meniran (*Phyllanthus niruri*), were discussed and their antibacterial activities were compared. Characterization by means of X-ray diffraction (XRD), Fourier transform infrared (FTIR), and field emission-scanning electron microscopy/energy dispersive X-ray spectroscopy (FE-SEM/EDS) were used to confirm the successful formation of n-ZnO using both plant extracts. The antibacterial activity of the n-ZnO synthesized from two different plant extracts was tested against* Klebsiella pneumoniae *and methicillin-resistant* Staphylococcus aureus *(MRSA). The results show that both n-ZnO has antibacterial activity against MRSA. Minimum inhibitory concentration (MIC) and minimum bactericidal concentration (MBC) values for n-ZnO synthesized from meniran extract were 78 and 156 mg/mL, respectively, while MIC and MBC values for n-ZnO synthesized from lavender extract were 156 and 312 mg/mL, respectively. These results confirm that the n-ZnO prepared from meniran extract is more effective in inhibiting MRSA than the n-ZnO prepared from lavender extract. This study proves that plant-based n-ZnO has anti-microbial activities and may serve as antimicrobial therapeutics.*

Keywords: *lavender; meniran; n-ZnO; MRSA,* Klebsiella pneumoniae

■ INTRODUCTION

The increasingly advanced development of science and technology has an impact on the birth of future technology, and it is nanotechnology. They are being represented as fundamental building blocks of future technology, and these materials will give new advanced properties. The diverse applications of this future technology provide a lot of attention in various fields including biology, medicine, energy, pharmaceuticals, food industry, and agriculture. Nanoparticles are one of the right approaches in developing nanotechnology [1].

Bacterial infection diseases are serious health problems that are considered as a threat to human health around the world. This also has an impact on the economic and social sectors. Increased outbreaks and infections of pathogenic bacteria, bacterial antibiotic resistance, the emergence of new mutated bacteria, bacterial infections in hospitals, and the lack of suitable vaccines in developing countries constitute a global health hazard for humans, especially children. Some examples are methicillin-resistant *Staphylococcus aureus* (MRSA) and *Klebsiella pneumonia* infections in

contaminated food and drinks. MRSA is a variant of the *S. aureus* bacteria, which has virulent characteristics, is resistant to many antibiotics, and often causes nosocomial infections in hospitalized patients [2]. *K. pneumonia* is the main bacteria that causes pneumonia, which is the largest cause of death among children [3]. Thus, the development of antibacterial nanotechnology needs to be carried out to reduce bacterial infectious diseases caused by contaminated food and drink.

Metal oxide nanoparticles are more interesting to research because they show several physical properties such as dimensions, uniform size distribution, morphology, and crystallinity, as well as better chemical properties compared to large or bulk materials [4]. Zinc oxide nanostructures (n-ZnO) are among the most popular metal oxide nanoparticles because they are non-toxic, biocompatible, and easy surface functionalization [5]. n-ZnO are versatile semiconductors that display significant optical transparency and luminescent properties in UV-visible regions [6]. n-ZnO has drawn interest in past two-three years due to its wide range of applications in the field of optoelectronics, optics, and biomedical systems. The most common technique in synthesizing n-ZnO is the chemical approach, such as sol-gel, hydrothermal, spray pyrolysis, microwave-assisted techniques, chemical vapor deposition, ultrasonic approach, and precipitation methods [6]. These approaches suffer from high energy demand and use chemicals during the process that have a toxic impact on the environment and allow the occurrence of dangerous side products from reactions, so a more environmentally friendly synthesis technique is urgently required [7].

Recently, green synthesis of nanoparticles from plant extracts has received much attention from researchers because it uses less toxic materials that can produce similar products. Green synthesis nanoparticles is an approach of synthesizing nanoparticles using microorganisms and plants having biomedical applications. It includes synthesis through part of the plants (roots, leaves, stems, seeds, or fruits), bacteria, fungi, algae, etc. Green synthesis methods are becoming the most preferred methods as they single step, clean, safe, and cost-effective. Biosynthetic routes provide nanoparticles of better-defined sizes and morphology as compared to other physical methods [8-10].

The natural strains and plant extract secrete some phytochemical compounds such as polyphenols, flavonoids, terpenoids, and phenolic acids, which can be used as reducing and capping agents in the synthesis of metal oxide nanoparticles, so they can replace the need for reducing agents from hazardous materials [11]. The extract of lavender plant (*Lavandula angustifolia*) and meniran leaves (*Phyllanthus niruri*) are natural ingredients that contain many essential compounds and have been used as medicine for a long time. Lavender extract contains linalool and linalyl acetate as good antibacterial and antioxidant agents [12]. The medicinal activities of *P. niruri* include antihypatotoxicity, antidiabetic, and antimicrobial activities with its compounds, such as alkaloids, tannins, and flavonoids [13]. Compared to lavender extract, the study on the utilization of meniran extract in synthesizing n-ZnO and then applied as antibacterial agent is still limited. Anbuvannan et al. [14] synthesized n-ZnO using meniran extract and zinc nitrate as precursor and then used as the photocatalyst. Therefore, this study explores the use of plant-derived n-ZnO for antibacterial application. All n-ZnO was prepared using biosynthesis approach from two kinds of plant extract (*L. angustifolia* and *P. niruri*) and then both plant-derived n-ZnO were tested against MRSA and *K. pneumonia*.

■ EXPERIMENTAL SECTION

Materials

There were two different plants used in this study; lavender plants and meniran leaves. The chemicals used to prepare n-ZnO in this research were zinc acetate dihydrate ($Zn(CH_3COO)_2{\cdot}2H_2O$) and 2 M sodium hydroxide (NaOH) solution. Sodium carbonate (Na_2CO_3), gallic acid, Folin-Ciocalteu, aluminium trichloride ($AlCl_3$), quercetin, and methanol were used for the determination of total phenolic and flavonoid content. Dimethyl sulfoxide (DMSO) solution, absolute ethanol (C_2H_5OH), 70% alcohol, Brain-heart Infusion (BHI) broth and agar media, McFarland standard 0.5, sodium chloride (NaCl), suspension of MRSA and *K.*

pneumoniae bacteria, distilled water, and universal pH paper were used for antibacterial assessment.

Instrumentation

Plant extraction and preparation of n-ZnO were performed using laboratory glassware (Pyrex) and a hotplate magnetic stirrer (IKA C-Mag HS7). The n-ZnO was dried using oven (Memmert UN55) and furnace (Nabertherm 30-3000). The characterization instruments used in this study were XRD (PANalytical AERIS), FTIR (Shimadzu IR Prestige-21), and FE-SEM/EDS (Hitachi SU-3500).

Procedure

Preparation of lavender extract

The dried lavender was refined using a blender to become powder. The lavender extract was made by dissolving 2 g of plant powder in 100 mL of distilled water. The solution was stirred and heated at 70 °C for 30 min. The lavender extract was cooled and filtered using Whatman filter paper No. 1. Then the filtrate obtained was stored at 2 °C for subsequent experimental uses.

Preparation of meniran extract

Ten grams of meniran leaves powder were mixed with 100 mL of distilled water and boiled at 100 °C for 10 min. The leaves powder mixture was then filtered using Whatman filter paper No. 1, and the filtrate was stored at 4 °C to prepare n-ZnO.

Preparation of n-ZnO from lavender extract

The preparation of n-ZnO from lavender extract was carried out based on the literature with slight modifications [15]. Briefly, 5 mL of lavender extract was added to 50 mL of $Zn(CH_3COO)_2{\cdot}2H_2O$ 0.75 M. The pH of the solution was 6 and then adjusted to 10 by adding dropwise of 2 M NaOH. The solution was kept stirred and heated at 70 °C for 30 min. The change in color from brownish yellow to yellowish white indicated the formation of n-ZnO. The mixture solution was then collected via decantation and filtered using Whatman filter paper No 1. The precipitate was washed with distilled water to remove residuals. The purified precipitate was dried at 70 °C in a hot air oven for 4 h, then calcined at 400 °C for 30 min. The material was mashed in a mortar pestle and stored at room temperature for further characterizations and applications.

Preparation of n-ZnO from meniran extract

The method of n-ZnO preparation was performed according to previous studies [13,16], with some modifications. $Zn(CH_3COO)_2$ 0.2 M in 50 mL of distilled water was stirred for 10 min. Meniran leaf extract was then titrated at about 2.5 mL for 2 h under a continuous stirring process at a temperature of 60 °C. The mixture pH was maintained at 12 by adding NaOH 0.1 M. The mixture was centrifuged at 6,000 rpm for 5 min and washed with distilled water. The residue was dried overnight in the hot air oven at 60 °C to yield a pale white color n-ZnO and then calcined at 400 °C for 30 min.

Determination of total phenolic and total flavonoid

The Folin-Ciocalteu method was used to determine total phenolic content (TPC) using gallic acid standard solution [17-18]. About 5 mg of plant extract was diluted in 5 mL of methanol and then 20% of Na_2CO_3 was added to 1 mL of this diluted extract and left for 2 h at room temperature. The absorbance of this mixture was then measured using UV-vis spectrophotometer at a wavelength of 765 nm. The total phenolic content was obtained as mg/g gallic acid of the plant extract.

The total flavonoid content (TFC) was determined using a standard curve with quercetin as the standard [19-20]. Diluted plant extract was added with $AlCl_3$ in methanol and NaOH 1 M. This mixture was then measured using UV-vis spectrophotometer at a wavelength of 510 nm. The flavonoid content was expressed as mg of quercetin equivalents (QE)/100 g of plant extract.

Antibacterial activity

The minimum inhibitory concentration (MIC) assay is used to determine the inhibitory effect of the synthesized n-ZnO on the growth of the bacteria. The method used to determine the MIC was microdilute. First, samples were prepared by dissolving the n-ZnO with DMSO at a 500 mg/mL concentration. The bacteria that will be tested, *K. pneumoniae* and MRSA, were

prepared by dissolving them in NaCl solution and increasing their concentration to 10^8 colony-forming units, then their turbidity was compared to the standard (McFarland 0.5). Microtitration 96-well plates were used in this method, and 100 µL of BHI broth media was titrated in wells 1–10 (from top to bottom). The sample was titrated at 100 µL in the first well. Suspension from the first well was then pipped up and titrated into the second well, then this treatment was carried out until the 10^{th} well and the last suspension was discarded. Next, each bacteria was titrated at 100 µL into the 1^{st}–10^{th} well, then homogenized by a micropipette. All the wells were closed and incubated at 37 °C for 24 h. Afterward, the wells were observed for clarity and turbidity. The MIC value was the one with the least concentration and had the highest clarity in the suspension.

The minimum bactericidal concentration (MBC) assay was the next part after the MIC assay to determine the antibacterial activity of the n-ZnO sample. This method used broth suspension from the well that showed the best MIC value. The broth suspension was streaked onto BHI agar media and incubated at 37 °C for 24 h. The MBC value was shown by preventing the growth of the bacteria on the BHI broth media.

■ RESULTS AND DISCUSSION

Plant-derived n-ZnO were formed through a chemical reaction between a $Zn(CH_3COO)_2$ solution with two different plant extracts at basic condition. The reaction between mixing solutions of $Zn(CH_3COO)_2$ and NaOH will produce $Zn(OH)_2$, CH_3COONa, and H_2O, as shown in Eq. (1). The formation of $Zn(OH)_2$ begins with the formation of a transparent turbid solution and then in Eq. (2) the mixture becomes milky white, forming a colloid. Excessed OH^- ions will react with $Zn(OH)_2$ to form the $[Zn(OH)_4]^{2-}$ complex and dissociate again to form Zn^{2+} and OH^- ions listed in Eq. (3). ZnO is formed in Eq. (4) through the heating process of $Zn(OH)_2$ [16]. The chemical reaction for the formation of ZnO from the process of mixing $Zn(CH_3COOH)_2{\cdot}2H_2O$ with NaOH is shown in Eq. (1-4).

$$Zn(CH_3COO)_2 \cdot 2H_2O + 2NaOH \rightleftharpoons Zn(OH)_2 + 2CH_3COONa + 2H_2O \quad (1)$$

$$Zn^{2+} + 2OH^- \rightleftharpoons Zn(OH)_2 \quad (2)$$

$$Zn^{2+} + 4OH^- \rightleftharpoons \left[Zn(OH)_4\right]^{2-} \quad (3)$$

$$Zn(OH)_2 \rightleftharpoons ZnO + H_2O \quad (4)$$

The proposed reaction of n-ZnO formation can be seen in Fig. 1, as adapted from Nurbayasari and Saridewi [21]. The n-ZnO was synthesized by plant extracts (lavender and meniran) which contribute as a stabilizer and capping agent.

Lavender and meniran extract contain phytochemicals or biological active components. This study determined the phytochemical compounds of phenolic (TPC) and flavonoid (TFC) from both extracts. The results show the lavender extract contained 165.1 mg/g of flavonoid and 77.1 mg/g of phenolic, while meniran extract contained 115.7 mg/g of flavonoid and 352.2 mg/g of phenolic. The results confirm that lavender extract contains higher flavonoid concentrations, while meniran extract contains higher phenolic concentrations. These biological active components from lavender and meniran extract were used in the reduction process of Zn^{2+} ions to Zn^0. The Zn^0 atoms were grouped and made a cluster, and then the particle growth and size were affected by their growth rate. Functional groups from the lavender and meniran components interact with the zinc surface, making a capper in the Zn^0 cluster called capping. The function of the capping agent is to prevent aggregation between clusters and make a stable n-ZnO. In binding the Zn^0 cluster, hydroxy groups also play a role, so the surface of

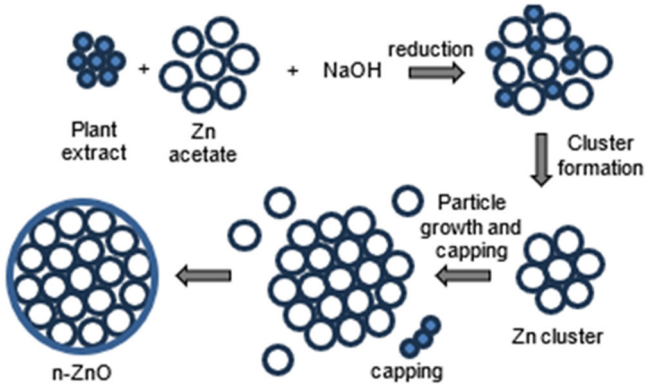

Fig 1. Scheme of the n-ZnO formation using plant (lavender and meniran) extracts

the particle is covered by negatively charged ions. Due to the presence of negative charges, there was a repulsive force between negative charges that prevented aggregation between nanoparticles [22].

XRD Patterns of n-ZnO

XRD characterization aims to determine the crystallinity of the material, the type of crystals, and the crystal size of the material formed. The diffractogram obtained from the OriginPro shows that the peaks detected at 2θ range from 30–80°. The data obtained from the characterization was then compared with the Miller Index on Crystallography Open Database (COD). Fig. 2 shows the diffraction pattern of ZnO formed from lavender and meniran extracts.

XRD data is used to compare the intensity of the peaks in the diffractogram data measured from the sample with the peaks in the standard ZnO diffractogram. Based on the results obtained from the QualX, n-ZnO from meniran leaf extract shows that the phase formed is zincite and has a hexagonal crystal form. The corresponding COD data for n-ZnO is No. 00-900-4180. The crystal structure of n-ZnO from the lavender extract is wurtzite with a hexagonal shape. The results are in accordance with COD data No. 00-900-4178.

The average particle size is calculated using the Debye-Scherrer equation contained in Eq. (5);

$$D = \frac{K\lambda}{\beta \cos\theta} \quad (5)$$

where D is the average particle size (nm), K is Scherrer's constant, which is 0.9, λ is the wavelength of X-ray radiation, θ is the diffraction angle (Bragg), and β is full width at half maximum (FWHM). The analysis results obtained using OriginPro and Excel showed that the average crystalline size of n-ZnO from lavender extract was 19.827 nm with a crystallinity of 79.77%, while n-ZnO from meniran leaf extract was 19.363 nm with a crystallinity of 57.57%.

IR Spectra of n-ZnO

Analysis of functional groups for lavender and meniran extracts and the plant-based n-ZnO are shown on the FTIR spectra ranging from 400 to 4000 cm^{-1} (Fig. 3). For the extract spectrum in both lavender and meniran in Fig. 3(a) and Fig. 3(b), respectively, the broad peak at 3200–3600 cm^{-1} showed the hydroxyl group (OH) stretching vibration. A peak in the range 1550–1650 cm^{-1} can be defined as C=C vibration, at the lavender extract could be the frequency of linalool and linalool acetate vibration [23]. Thus, in meniran extract, this range peak was the cycloalkene showing the existence of polyphenol groups. Linalool and polyphenol in the extract were important capping agents for forming $Zn(OH)_2$. The synthesized n-ZnO from the lavender and meniran spectra in Fig. 3(c) and 3(d) showed no difference in peaks. The peaks of OH groups can be seen at 3200–3600 cm^{-1}, and the wavenumber at 1300–1400 cm^{-1} was defined as the stretching vibration of C–O–H functional groups. The vinyl group ($RHC=CH_2$) was shown at 1635–1650 cm^{-1}. The spectrum

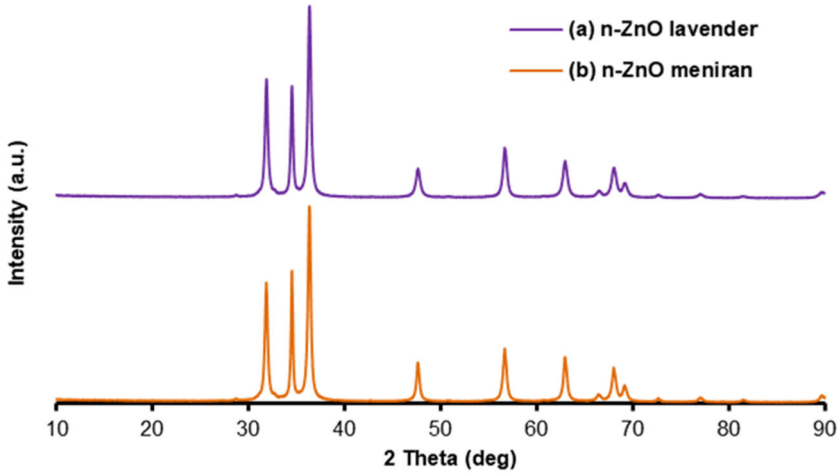

Fig. 2. X-ray diffractogram of n-ZnO from the (a) lavender and (b) meniran extract

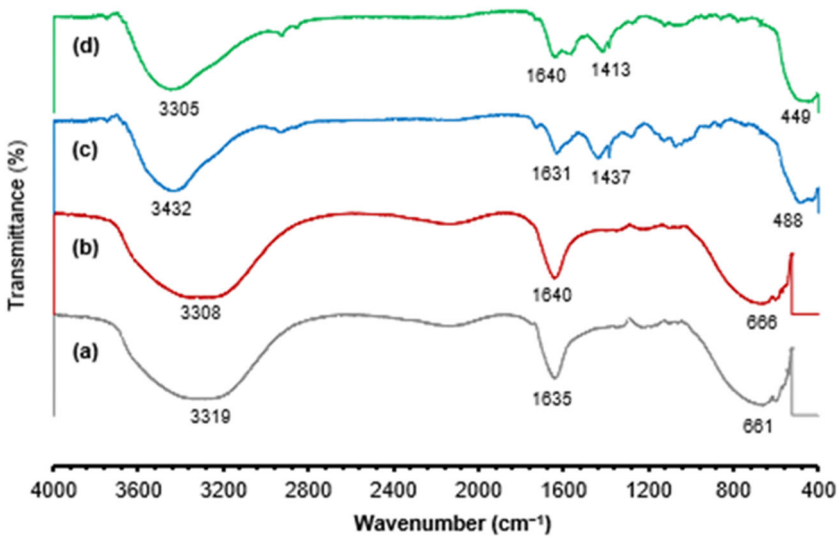

Fig 3. IR spectrum of the (a) lavender (b) meniran extract, (c) n-ZnO-lavender, and (d) n-ZnO-meniran

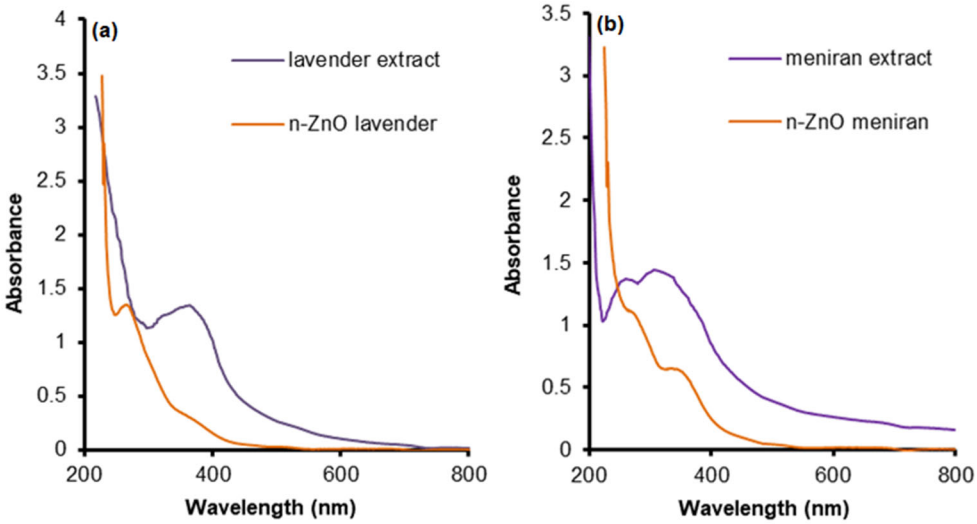

Fig 4. UV-vis spectra analysis of n-ZnO from (a) lavender and (b) meniran extract

of Zn–O bond presence was assigned at the fingerprint zone (< 700 cm^{-1}). In this spectrum, the Zn-O peak was shown at 400–500 cm^{-1} [24]. Those spectra confirmed that both lavender and meniran, with their phytochemicals like alkaloid, terpenoid, and phenolic, had contributed to stabilizing the n-ZnO synthesis. These results were supported by previous studies [25-27].

UV-vis Studies of n-ZnO

The plant extract and the resulting n-ZnO were characterized using a UV-vis spectrophotometer to determine the maximum wavelength. The wavelength used in this characterization is 200–800 nm. Fig. 4(a) and 4(b) show the results of measuring the maximum wavelength of lavender extract, meniran extract, and n-ZnO produced from each extract.

The results of UV-vis measurements of lavender extract showed a typical absorption peak at a maximum wavelength of 364 nm and an absorbance value of 0.48, while the results of UV-vis measurements of meniran leaf extract showed a typical absorption peak at a maximum wavelength of 376 nm and an absorbance value of 0.49. The absorption peaks in lavender extract and meniran leaf extract predict that lavender and meniran leaf contain secondary metabolites such as alkaloids, flavonoids, and tannins.

The appearance of an absorption peak at a maximum wavelength of 260 nm and an absorbance value of 0.6 indicates that n-ZnO from the lavender extract was successfully formed. The appearance of an absorption peak at a wavelength of 260 nm predicts that n-ZnO has an surface plasmon resonance (SPR) phenomenon [28]. The maximum absorbance of n-ZnO from meniran leaf extract is at a wavelength of 335 nm, which is close to the research result of Saravanan [13], where ZnO resulting from green synthesis with meniran leaf extract has a maximum absorption at a wavelength of 369 nm.

Morphological Studies of n-ZnO

The FESEM image of synthesized n-ZnO lavender was given in Fig. 5(a) and n-ZnO meniran was given in Fig. 5(b). These figures confirm that the n-ZnO lavender has the shape of a nanocube while n-ZnO meniran has the shape of a truncated hexagonal. The average size of n-ZnO was analyzed using the ImageJ application by collecting 50 size data points of n-ZnO. Then, the data were input into the OriginPro application, resulting in the histogram in Fig. 6. Based on the calculation, the average particle size for n-ZnO lavender is 80.27 nm, and for n-ZnO meniran is 71.12 nm.

The average particle size obtained shows that the n-ZnO size was in the nanomaterial category (0–100 nm). But, as shown in Fig. 6, there were still particles exceeding 100 nm. Agglomeration can be the cause of this large size. Moreover, FESEM/EDS was used to analyze the purity of n-ZnO. Fig. 7 shows the results from EDS of n-ZnO lavender and meniran. From the results, there were two peaks, which were zinc and oxygen elements. The n-ZnO lavender is composed of 52.0% zinc and 48.0% oxygen, and n-ZnO meniran is

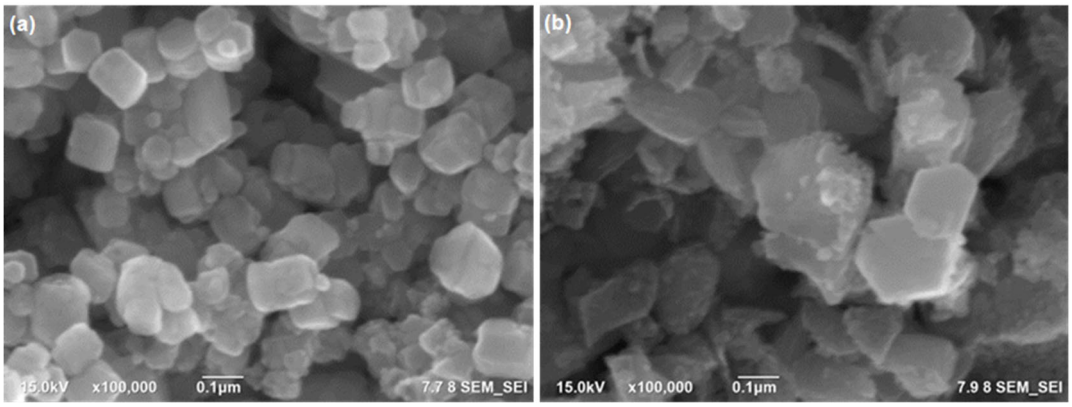

Fig 5. FESEM image of n-ZnO (a) lavender and (b) meniran

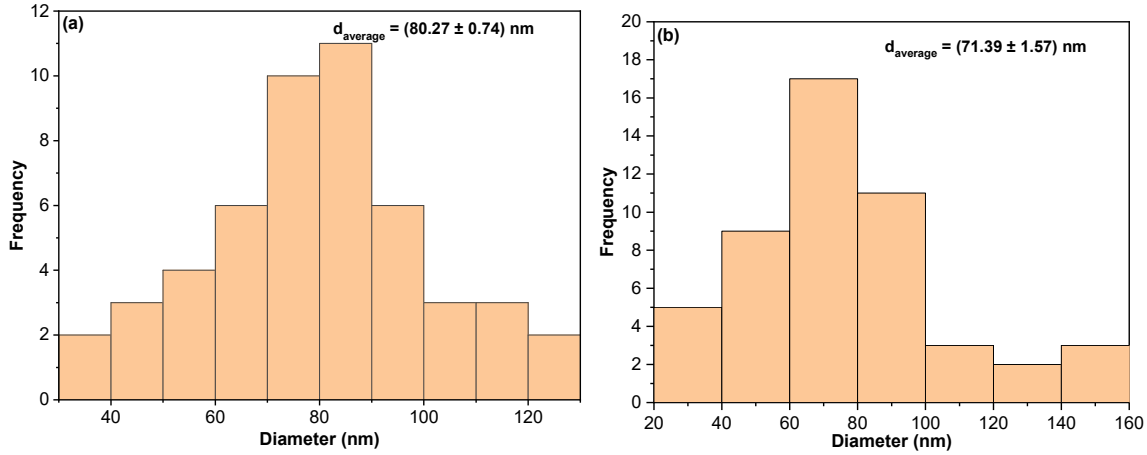

Fig 6. Histogram average particle size of n-ZnO prepared from (a) lavender and (b) meniran extracts

composed of 53.0% zinc and 47.0% oxygen. This result confirmed that there are no impurities in synthesized n-ZnO, both in lavender and meniran.

Antibacterial Activity of n-ZnO

Antibacterial activity tests were carried out using the microdilution method because it has a higher level of sensitivity than other methods. The microdilution technique is used to calculate the MIC and MBC. The calculation is based on turbidity, which indicates the presence of bacterial growth and clarity, that is the absence of bacterial growth which can be seen after incubation for 24 h at a temperature of 37 °C. The results of antibacterial testing using the microdilution technique are shown in Table 1. The antibacterial activity of n-ZnO from meniran leaf extract is more effective than n-ZnO from lavender extract, as seen from the MIC value against MRSA bacteria, which is 78.12 μg/mL. In order to study the effect of plant extract on the antibacterial properties, the antibacterial activity of the lavender and meniran extract were conducted against MRSA and *K. pneumonia*. The results in Table 1 show that both plant extracts do not have antibacterial properties (> 500 μg/mL), confirming the antibacterial activity of the n-ZnO lavender and n-ZnO meniran due to the ZnO nanostructured.

The antibacterial activity of n-ZnO has been referred to several issues, but the exact inhibition mechanism is not completely illuminated and is still controversial. There are some possible distinctive mechanisms, such as direct contact of n-ZnO with cell walls, resulting in destructing bacterial cell, liberation of antimicrobial ions mainly Zn^{2+} ions, and reactive oxygen species (ROS) formation. The shape and size of n-ZnO affect the ability of the n-ZnO to penetrate into cell walls of bacteria and the biocidal activity [29]. In this study, the antibacterial activity of the n-ZnO synthesized using meniran extract against MRSA is higher than n-ZnO prepared using lavender extract. This antibacterial activity may be due to the particulate ZnO releases of free Zn^{2+} ions that are toxic to the bacteria. The other proposed mechanism of bacterial inhibition is due to the size of the n-ZnO. The n-ZnO prepared using meniran extract is smaller than the n-ZnO prepared using lavender extract. Smaller-sized n-ZnO can easily penetrate into bacterial membranes due to their large interfacial area, thus enhancing their antibacterial activity [29-30].

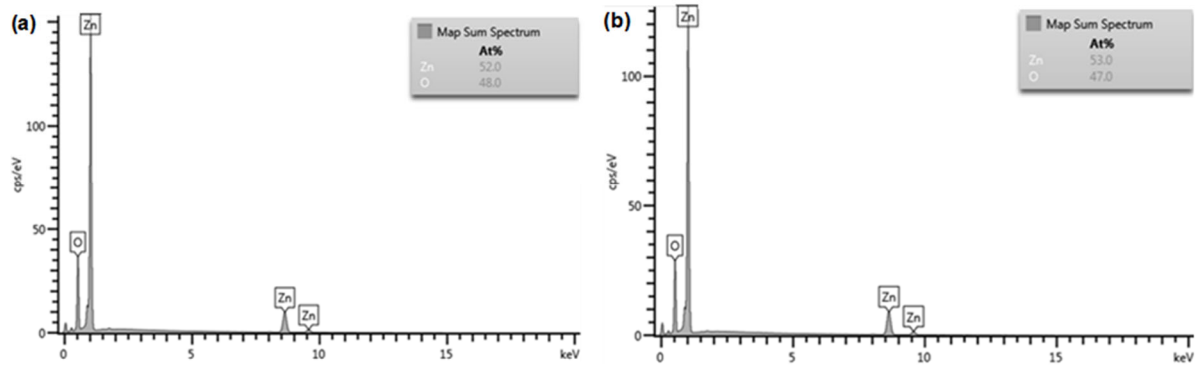

Fig 7. EDS image of n-ZnO synthesized using (a) lavender and (b) meniran extract

Table 1. Antibacterial activity of plant-based n-ZnO

Compound	MRSA		*Klebsiella pneumonia*	
	MIC (μg/mL)	MBC (μg/mL	MIC (μg/mL)	MBC (μg/mL)
n-ZnO lavender	156.25	312.5	> 625	1250
n-ZnO meniran	78.12	156.25	625	625
Lavender extract	> 500	> 500	> 500	> 500
Meniran extract	> 500	> 500	> 500	> 500

■ CONCLUSION

The green synthesis of n-ZnO from two kinds of plant extract, lavender (*Lavandula angustifolia*) and meniran (*Phyllanthus niruri*), has been successfully conducted in this study. The results confirm that green synthesis of n-ZnO using plants such as lavender and meniran has a promising potential because it is pollution-free and eco-friendly, thus supporting the sustainability environment. The phytochemical and biologically active compounds in lavender and meniran extract can be used as capping agents as well as stabilizers for the synthesis of n-ZnO. The antibacterial activity of green synthesized n-ZnO in both lavender and meniran were also assessed. The results showed high antibacterial activity, as proven by their MIC and MBC values. Rather than n-ZnO lavender, n-ZnO meniran has better antibacterial activity, as proven by the small MIC and MBC values. It highlights the potential application of n-ZnO in biomedical fields, as antibacterial or therapeutic agents.

■ ACKNOWLEDGMENTS

The authors gratefully acknowledge to National Research and Innovation Agency (BRIN) for providing facilities, scientific, and technical support through E-*layanan Sains (ELSA)* BRIN and LPDP-BRIN through the *Riset dan Inovasi untuk Indonesia Maju (RIIM)* 2023 research grant (No. 12/II.7/HK/2023) for providing funding for this project.

■ CONFLICT OF INTEREST

All the authors have declared that there is no conflict of interest.

■ AUTHOR CONTRIBUTIONS

Dhiya Fakhirah: data curation and writing. Tya Aisha Maghfira: data curation and writing. Aulia Sukma Hutama: supervision and review. Abdi Wira Septama: Methodology, data curation, review, and editing. Faiza Maryani: data curation, review. Fransiska Sri Herwahyu Krismastuti: main contributor, conceptualization, methodology, data curation, supervision, writing, review, editing and funding.

■ REFERENCES

[1] Ajitha, B., Ashok Kumar Reddy, Y., and Sreedhara Reddy, P., 2015, Green synthesis and characterization of silver nanoparticles using *Lantana camara* leaf extract, *Mater. Sci. Eng., C*, 49, 373–381.

[2] Santosaningsih, D., Erikawati, D., Hakim, I.A., Santoso, S., Hidayat, M., Suwenda, A.H., Puspitasari, V., Irhamni, I., Kuntaman, K., van Arkel, A.L.E., Terlouw, L.G., Oudenes, N., Willemse-Erix, D., Snijders, S.V., Erler, N.S., Verbrugh, H.A., and Severin, J.A., 2019, Reducing transmission of methicillin-resistant *Staphylococcus aureus* in a surgical ward of a resource-limited hospital in Indonesia: An intervention study, *Infect. Prev. Pract.*, 1 (3-4), 100028.

[3] UNICEF, 2019, *One child dies of pneumonia every 39 seconds, agencies warn*, https://www.unicef.org/indonesia/press-releases/one-child-dies-pneumonia-every-39-seconds-agencies-warn, accessed on April 11, 2023.

[4] Saravanadevi, K., Kavitha, M., Karpagavinayagam, P., Saminathan, K., and Vedhi, C., 2022, Biosynthesis of ZnO and Ag doped ZnO nanoparticles from *Vitis vinifera* leaf for antibacterial, photocatalytic application, *Mater. Today: Proc.*, 48, 352–356.

[5] Preethi, S., Abarna, K., Nithyasri, M., Kishore, P., Deepika, K., Ranjithkumar, R., Bhuvaneshwari, V., and Bharathi, D., 2020, Synthesis and characterization of chitosan/zinc oxide nanocomposite for antibacterial activity onto cotton fabrics and dye degradation applications, *Int. J. Biol. Macromol.*, 164, 2779–2787.

[6] Agarwal, H., Venkat Kumar, S., and Rajeshkumar, S., 2017, A review on green synthesis of zinc oxide nanoparticles – An eco-friendly approach, *Resour.-Effic. Technol.*, 3 (4), 406–413.

[7] Salnus, S., Wahab, W., Arfah, R., Zenta, F., Natsir, H., Muriyati, M., Fatimah, F., Rajab, A., Armah, Z., and Irfandi, R., 2022, A review on green synthesis, antimicrobial applications and toxicity of silver

nanoparticles mediated by plant extract, *Indones. J. Chem.*, 22 (4), 1129–1143.

[8] Fakhari, S., Jamzad, M., and Kabiri Fard, H., 2019, Green synthesis of zinc oxide nanoparticles: A comparison, *Green Chem. Lett. Rev.*, 12 (1), 19–24.

[9] Bandeira, M., Giovanela, M., Roesch-Ely, M., Devine, D.M., and da Silva Crespo, J., 2020, Green synthesis of zinc oxide nanoparticles: A review of the synthesis methodology and mechanism of formation, *Sustainable Chem. Pharm.*, 15, 100223.

[10] Pillai, A.M., Sivasankarapillai, V.S., Rahdar, A., Joseph, J., Sadeghfar, F., Anuf, R., Rajesh, K., and Kyzas, G.Z., 2020, Green synthesis and characterization of zinc oxide nanoparticles with antibacterial and antifungal activity, *J. Mol. Struct.*, 1211, 128107.

[11] Izadiyan, Z., Shameli, K., Miyake, M., Hara, H., Mohamad, S.E., Kalantari, K., Mohd Taib, S.H., and Rasouli, E., 2020, Cytotoxicity assay of plant-mediated synthesized iron oxide nanoparticles using *Juglans regia* green husk extract, *Arabian J. Chem.*, 13 (1), 2011–2023.

[12] Rather, G.A., Nanda, A., Raj, E., Mathivanan, N., and Nayak, B.K., 2022, Green synthesis of ZnO nanoparticles using the leaf extract of *Lavandula angustifolia* and evaluation of their antibacterial activity against human pathogens, *Int. J. Health Sci.*, 6 (S2), 13478–13485.

[13] Ramesh, P., and Saravanan, K., 2018, Green synthesis, characterization, antimicrobial and food packaging application of biocompatible zinc oxide nanoparticles, *Asian J. Res. Pharm. Sci. Biotechnol.*, 6 (4), 76–86.

[14] Anbuvannan, M., Ramesh, M., Viruthagiri, G., Shanmugam, N., and Kannadasan, N., 2015, Synthesis, characterization and photocatalytic activity of ZnO nanoparticles prepared by biological method, *Spectrochim. Acta, Part A*, 143, 304–308.

[15] Naiel, B., Fawzy, M., Halmy, M.W.A., and Mahmoud, A.E.D., 2022, Green synthesis of zinc oxide nanoparticles using Sea Lavender (*Limonium pruinosum* L. Chaz.) extract: Characterization, evaluation of anti-skin cancer, antimicrobial and antioxidant potentials, *Sci. Rep.*, 12 (1), 20370.

[16] Noorjahan, C.M., 2019, Green synthesis, characterization and antibacterial activity of zinc oxide nanoparticles, *Asian J. Pharm. Clin. Res.*, 12 (4), 106–110.

[17] Meda, A., Lamien, C.E., Romito, M., Millogo, J., and Nacoulma, O.G., 2005, Determination of the total phenolic, flavonoid and proline contents in Burkina Fasan honey, as well as their radical scavenging activity, *Food Chem.*, 91 (3), 571–577.

[18] Tohidi, B., Rahimmalek, M., and Arzani, A., 2017, Essential oil composition, total phenolic and flavonoid contents, and antioxidant activity of *Thymus* species from different regions of Iran, *Food Chem.*, 220, 153–161.

[19] Saeed, N., Khan, M.R., and Shabbir, M., 2012, Antioxidant activity, total phenolic and total flavonoid contents of whole plant extracts *Torilis leptophylla* L, *BMS Complement. Altern. Med.*, 12 (1), 221.

[20] Aryal, S., Baniya, M.K., Danekhu, K., Kunwar, P., Gurung, R., and Khoirala, N., 2019, Total phenolic content and antioxidant potential of wild vegetables from Western Nepal, *Plants*, 8 (4), 96.

[21] Nurbayasari, R., and Saridewi, N., 2017, Biosintesis dan karakterisasi nanopartikel ZnO dengan ekstrak rumput laut hijau *Caulerpa* sp., *Jurnal Perikanan Universitas Gadjah Mada*, 19 (1), 17–28.

[22] Tournebize, J., Boudier, A., Joubert, O., Eidi, H., Bartosz, G., Maincent, P., Leroy, P., and Sapin-Minet, A., 2012, Impact of gold nanoparticle coating on redox homeostasis, *Int. J. Pharm.*, 438 (1-2), 107–116.

[23] Agatonovic-Kustrin, S., Kustrin, E., Gegechkori, V., and Morton, D.W., 2020, Anxiolytic terpenoids and aromatherapy for anxiety and depression, *Adv. Exp. Med. Biol.*, 1260, 283–296.

[24] Shafique, S., Jabeen, N., Ahmad, K.S., Irum, S., Anwaar, S., Ahmad, N., Alam, S., Ilyas, M., Khan, T.F., and Hussain, S.Z., 2020, Green fabricated zinc oxide nanoformulated media enhanced callus

induction and regeneration dynamics of *Panicum virgatum* L., *PLoS One*, 15 (7), e0230464.

[25] Chabattula, S.C., Gupta, P.K., Tripathi, S.K., Gahtori, R., Padhi, P., Mahapatra, S., Biswal, B.K., Singh, S.K., Dua, K., Ruokolainen, J., Mishra, Y.K., Jha, N.K., Bishi, D.K., and Kesari, K.K., 2021, Anticancer therapeutic efficacy of biogenic Am-ZnO nanoparticles on 2D and 3D tumor models, *Mater. Today Chem.*, 22, 100618.

[26] Dulta, K., Koşarsoy Ağçeli, G., Chauhan, P., Jasrotia, R., and Chauhan, P.K., 2021, A novel approach of synthesis zinc oxide nanoparticles by *Bergenia ciliata* rhizome extract: Antibacterial and anticancer potential, *J. Inorg. Organomet. Polym. Mater.*, 31 (1), 180–190.

[27] Faisal, S., Jan, H., Shah, S.A., Shah, S., Khan, A., Akbar, M.T., Rizwan, M., Jan, F., Wajidullah, W., Akhtar, N., Khattak, A., and Syed, S., 2021, Green synthesis of zinc oxide (ZnO) nanoparticles using aqueous fruit extracts of *Myristica fragrans*: Their characterizations and biological and environmental applications, *ACS Omega*, 6 (14), 9709–9722.

[28] Chikkanna, M.M., Neelagund, S.E., and Rajashekarappa, K.K., 2018, Green synthesis of zinc oxide nanoparticles (ZnO NPs) and their biological activity, *SN Appl. Sci.*, 1 (1), 117.

[29] Sirelkhatim, A., Mahmud, S., Seeni, A., Mohamad Kaus, N.H., Ann, L.C., Mohd Bakhori, S.K., Hasan, H., and Mohamad, D., 2015, Review on zinc oxide nanoparticles: Antibacterial activity and toxicity mechanism, *Nano-Micro Lett.*, 7 (3), 219–242.

[30] Mendes, C.R., Dilarri, G., Forsan, C.F., Sapata, V.M.R., Lopes, P.R.M., de Moraes, P.B., Montagnolli, R.N., Ferreira, H., and Bidoia, E.D., 2022, Antibacterial action and target mechanisms of zinc oxide nanoparticles against bacterial pathogens, *Sci. Rep.*, 12 (1), 2658.